Removal of crystal violet from aqueous solution using environment-friendly and water-resistance membrane based on polyvinyl/agar/maltodextrin

Article *in* Materials Today: Proceedings · December 2020

DOI: 10.1016/j.matpr.2020.09.391

CITATIONS
0

READS
23

4 authors, including:

Bich Ngoc Hoang
Nguyen Tat Thanh University
9 PUBLICATIONS **87** CITATIONS

SEE PROFILE

Thuong Thi Nguyen
University of Sciences
40 PUBLICATIONS **250** CITATIONS

SEE PROFILE

Materials Today: Proceedings xxx (xxxx) xxx

Contents lists available at ScienceDirect

Materials Today: Proceedings

journal homepage: www.elsevier.com/locate/matpr

Removal of crystal violet from aqueous solution using environment-friendly and water-resistance membrane based on polyvinyl/agar/maltodextrin

Bich Ngoc Hoang [a,b], Thuong Thi Nguyen [b,c,*], Dai Van Nguyen [d], Lam Van Tan [b]

[a] Faculty of Environment and Natural Resources, Ho Chi Minh City University of Technology, Ho Chi Minh City 700000, Viet Nam
[b] NTT Hi-Tech Institute, Nguyen Tat Thanh University, Ho Chi Minh City 700000, Viet Nam
[c] Center of Excellence for Green Energy and Environmental Nanomaterials (CE@GrEEN), Nguyen Tat Thanh University, Ho Chi Minh City 700000, Viet Nam
[d] Faculty of Automobile Technology, Van Lang University, 45 Nguyen Khac Nhu street, Co Giang ward, District 1, Ho Chi Minh City 700000, Viet Nam

ARTICLE INFO

Article history:
Received 30 June 2020
Received in revised form 17 August 2020
Accepted 16 September 2020
Available online xxxx

Keywords:
Adsorption
Crystal violet
Poly (vinyl alcohol)
Water-resistance membrane

ABSTRACT

In the past few decades, dye-based contamination has been considered as a severe environmental problem faced by many developing countries due to increasingly growth of textile industry. Carbon-based materials have found as an excellent adsorbent for organic species because of its porous structure. Conversely, the cost-inefficiency and the difficulty to collect them after use, is the mainly negative mark when applying them in the large-scale. Thus, the development of low-cost, facile processing and eco-friendly membranes with high performance and high adsorption capacity for dye-based pollutants should be considered as a very important and urgent task. Herein, we wish to report the application of poly (vinyl alcohol)-based blend membranes combined with agar and maltodextrin for the elimination of crystal violet (CV) in water media. These blend membranes were fabricated via the simple solvent casting process. Effect of different factors, e.g., contact time between adsorbents and adsorbates, solution pH, and initial crystal violet concentration on the uptake capacity of blend membrane was studied in batch model. The obtained results revealed that adsorption kinetic was well obeyed with Pseudo-second order model, which was mainly controlled by chemisorption process. Langmuir model still well-described for adsorption isotherm for crystal violet dye of poly (vinyl alcohol) membrane combined with agar and maltodextrin. The maximum amount of CV uptake by blend membrane was found to be 84.618 $mg{\cdot}g^{-1}$. These outcomes indicate a potential use of poly (vinyl alcohol)-based blend membranes combined with agar and maltodextrin for the elimination of CV in water media.

1. Introduction

Textile industry has made a great contribution to economic development in developing countries. However, a large amount of wastewater containing toxic organic residues resulting from different steps in the dyeing and finishing process was discharged without through treatment, which exerted negative effects on living things and their environment [1]. The presence of organic dyes in water may pose potential harm to human health because they are composed of complex aromatic structure resulting in difficulty to biodegrade. For instance, Crystal violet (CV) was warned as a cationic dye and a synthetic triphenylmethane dye, which is a proved carcinogenic agent, causing adverse eye irritation, toxic by inhalation and exposure [2]. Many physicochemical methods were documented to eliminate CV from water environment, i.e., chemical oxidation [3], adsorption [4–9], photo-catalysis [10,11], and membrane filtration [12]. Among aforementioned methods, the adsorption was more in favor of the elimination of CV due to its simple handle and cost-efficacy. Activated carbon and clays

* Corresponding author at: NTT Hi-Tech Institute, Nguyen Tat Thanh University, Ho Chi Minh City 700000, Viet Nam.
E-mail address: nthithuong@ntt.edu.vn (T. Thi Nguyen).

https://doi.org/10.1016/j.matpr.2020.09.391
2214-7853/

provided were preferred for CV removal on account of its high adsorption capacity [4,13–16]. However, the utilization of such adsorbents was difficult to recovery and produced a large amount of sludge after decolonizing organic species [17,18]. The development of environment-friendly adsorbent with high effectiveness as well as easy to recovery after decoloring process was viable approach for CV removal.

Polyvinyl alcohol (PVA) is a product derived from partially hydrolysis of polyvinyl acetate. Although it was known as a synthetic polymer, it was used for textile, paper and food packaging industries thanks to its biocompatibility and biodegradability [19]. Nevertheless, the water-soluble character of PVA because of the high density of hydroxyl groups in matrix is a major drawback limiting its application in water purification. For the purpose of decreasing of hydrophilicity of PVA, many studies reported on crosslinking of hydroxyl groups via physical routine [20,21] and chemical routine [22–26]. In recent years, PVA-based hydrogel membrane were widely applied for removing textile dyes such as crystal violet [9,27–29]. For instance, the CV could be removed up to 98.6% by PVA/alginate/kaolin gel at initial concentration of 30 $mg{\cdot}L^{-1}$, pH 5, and 30 °C for 30 h [27]. The adsorption process of PVA/alginate/kaolin gel well obeyed to second-order kinetic. Papancea et al. [28] reported on the addition of natural polymers such as scleroglucan (Sl), microfibers of cellulose (Cl), and natural polysaccharide (Zein. Sl) into PVA and the adsorption capacity of so prepared cryogel membrane for CV was found in the following order as follows: PVA/Cl (13.13 $mg{\cdot}g^{-1}$) > PVA/Sl (1.93 $mg{\cdot}g^{-1}$) > PVA/Zein Sl (1.203 $mg{\cdot}g^{-1}$). However, such bio-insertion did not bring effectiveness because the adsorption capacity of so prepared cryogel membrane was lower compared to pure PVA membrane. A study on PVA/kappa-carrageenan nanocomposite hydrogels showed the maximum amount of CV uptake at 55 $mg{\cdot}g^{-1}$ [29]. The combination of magnetic Fe_3O_4 nanoparticles into PVA/kappa-carrageenan effectively contribute to recovery of adsorbents after use but it induced a reduction in the CV uptake (52 $mg{\cdot}g^{-1}$). Furthermore, Mansor et al. [9] showed that the combination of cellulose acetate revitalized the hydrophobicity of PVA membrane and provided selective adsorption for CV dye. The removal of crystal violet using PVA-based hydrogel membrane was widely investigated but not adequately.

In the present work, continuing our previous report on the preparation of composite membrane and their utilization for selective adsorption of Methylene Blue (MB) from water environment [30], we focused on the elimination of crystal violet (CV) by using high water-resistance PVA/agar/maltodextrin (20/40/40) membrane with higher CV adsorption capacity compared to MB removal. Furthermore, we also evaluated the effect of adsorption conditions (e.g., solution pH, contact time between adsorbates and adsorbents, and initial CV concentration) along with the kinetics and isotherms of adsorption process. The addition of agar and maltodextrin containing many hydroxyl groups was expected to form the crosslinking with hydroxyl groups of PVA to revitalize the hydrophobic property of the hydrogel membrane.

2. Experimental

2.1. Materials

Agar power was provided by BDH Prolabo (VWR Singapore, Ltd). Poly (vinyl alcohol) in cold water soluble (PVA, $(C_2H_4O)_n$, M_W - ~ 160,000 $g.mol^{-1}$, 85% hydrolyzed), crystal violet (CV; $C_{25}N_3H_{30}Cl$, 99.9%)), and maltodextrin ($C_{6n}H_{(10n+2)}O_{(5n+1)}$, average DE of 20) were supplied by Himedia. The experiments carried out in the simulated wastewater by adding organic dyes to distillation water.

2.2. Preparation of the PAM membranes

The blend films were prepared through simple solution casting as described previously [30]. Firstly, the aqueous solutions of PVA 2% (w/v), agar 4% (w/v), and maltodextrin 4% (w/v) were mixed in equal volume. The glycerol (30% wt/wt respect to total weight of PVA, agar, and maltodextrin) as a plasticizer was added into the film-forming solution under magnetic stirring at 70 °C for 1 h. Then, the film-forming solution was centrifuged to remove insoluble solids and impurities before casting on a polypropylene mold and drying at 45 °C for 48 h. The PVA film combined simultaneously with agar and maltodextrin was referred as PAM. The single addition of agar and maltodextrin into PVA was performed in the same way and marked as PA and PM, respectively.

2.3. Characterization

The structure and possibly chemical interaction between blended compositions in blend membranes were determined using ATR/ FTIR analysis on JASCO FT/IR-6000 equipment combined with ATR PRO ONE equipment in the wavelength ranged from 4000 cm^{-1} to 500 cm^{-1}. The surface morphology at micro-level and cross section images of membranes were measured on JSM-IT200 Scanning Electron Microscope equipment. The thermal property of membranes was determined using thermogravimetric analysis (TGA) on the Q500 analyser with a heating speed of 10 °C/min in N_2 environment.

2.4. Swelling degree

The swelling degree experiments were carried out following to the report of Jipa et al. [31] with a some changes. The 2 cm × 2 cm size membranes were dried at 75 °C for 24 h. The dried membrane was weighted to obtain first weight (m_i). The dried membranes were further immersed in distillation water at 27 °C for 6 days. The immersed membranes were taken off after each day and removed residue water on the surface before weighting to obtain the swollen weight of the specimen (m_f). The swelling degree was calculated by applying the following formula:

$$SD = \frac{m_i - m_f}{m_i} \times 100 \quad (1)$$

2.5. Adsorption experiments

Firstly, 0.1 g of PAM membrane was added in 100 mL of the CV aqueous solution at known solution pH and initial weight under shaking at 180 rpm. After certain time, the CV-loaded membranes were taken off and residual adsorbates was determined on the evolution 60 s UV – Vis spectrophotometer in the wavelength of 577 nm. Adsorption capacity (q_e) of membrane for CV was calculated based on the equation:

$$q_e = \frac{(C_0 - C_e).v}{m} \quad (2)$$

where C_o and C_e are the initial CV concentration and equilibrium concentration expressed in $mg.L^{-1}$ and $mg.L^{-1}$, respectively; v (L) is the volume of dye and m (g) is the dosage of adsorbent.

2.6. Point of zero charge (pH_z) determination

The pH_z was measured due to the method well-described in the previous report [32] with small change. Firstly, 0.1 g of PAM membrane was added into Erlenmeyer flask containing 50 mL of KCl 0.1 M at the initial pH series (pH_i) in the range of 2–10 adjusted by using NaOH and HCl. The mixture solution involved PAM membrane in Erlenmeyer flask was magnetically stirred for 10 min at

temperature (27 °C) before stabilizing for 24 h. The PAM membrane was then separated from mixture solution. The final solution pH values of mixture solution were further recorded and noticed as pH_f. The pH_z value was determined from the curve of pH_f vs pH_i at the point of $pH_i = pH_f$.

2.7. Adsorption kinetics and isotherms

The adsorption kinetic was studied in the non-linear models such as Pseudo-first order [33], Pseudo-second order [34], Elovich [35] and Bangham [36]. These models were respectively described in following formula:

$$q_t = q_e(1 - e^{-k_1 t}) \tag{3}$$

$$q_t = \frac{q_e^2 k_2 t}{1 + k_2 t q_e} \tag{4}$$

$$q_t = \frac{1}{\beta} ln(1 + \alpha\beta t) \tag{5}$$

$$q_t = k_B t^{\alpha_B} \tag{6}$$

where q_t and q_e are the adsorption capacity of adsorbent at time t and the adsorption capacity at the equilibrium expressed in unit of $mg{\cdot}g^{-1}$, k_1 and k_2 are the rate constant of the Pseudo-first order and the Pseudo-second order respectively expressed in unit of min^{-1} and $g.(mg{\cdot}min)^{-1}$, β is the desorption rate ($g{\cdot}mg^{-1}$), α is the rate of chemical absorption $(mg.(g{\cdot}min)^{-1})$, k_B and α_B are Bangham constants.

The adsorption isotherms were closely related to possibly consider the interaction between adsorbates and adsorbents in gas/liquid/solid interfaces. This may indicate that important parameters related to the adsorption mechanisms. Herein non-linear isotherm models such as Langmuir [37], Freundlich [38], Temkin [39], and Dubinin-Radushkevich (D-R) [39] were utilized to consider adsorption process. These models were described in the following formula:

$$q_e = \frac{q_m K_L C_e}{1 + K_L C_e} \left(R_L = \frac{1}{1 + K_L C_o}\right) \tag{7}$$

$$q_e = K_F C_e^{1/n} \tag{8}$$

$$q_e = B_T \ln(k_T C_e) \left(B_T = \frac{RT}{b}\right) \tag{9}$$

$$q_e = q_{DR} e^{-K_{DR}\varepsilon^2} \left(E = \frac{1}{\sqrt{2B}}; \varepsilon = R.T.\ln\left(1 + \frac{1}{C_e}\right)\right) \tag{10}$$

where q_m is the maximum amount of adsorbed CV and q_e is the amount of adsorbed CV at equilibrium expressed in $mg{\cdot}g^{-1}$, K_L is Langmuir constant expressed in $L.mg^{-1}$, R_L is dissociation coefficient with $R_L > 1$ (unfavorable), $R_L = 1$ (linear), $0 < R_L < 1$ (favorable) and $R_L = 0$ (not reversed). In the Freundlich equation, K_F is Freundlich constant expressed in $(mg{\cdot}g^{-1}).(L.mg^{-1})^n$ and 1/n is the uptake intensity with $n < 1$ (single-layer adsorption) and $n > 1$ (multi-layer adsorption). In the Temkin equation, k_T is correlated to the isotherm Temkin constant expressed in $L.g^{-1}$ and b is Temkin constant expressed in $L.mol^{-1}$. In DR equation, E is the adsorption energy expressed in $kJ.mol^{-1}$, ε is the Polanyi potential, and K_{DR} is the D-R constant expressed in $(Mol^2).(Kj^2)^{-1}$.

3. Result

3.1. The characterization of the membranes

The surface image at micro-level and cross-section morphology of neat PVA, PA, PM and PAM membrane were determined via SEM analysis as shown in Fig. 1. In general, the smooth, compact, and uniform surface with no cracks were observed for all membranes. However, there are some differences when looking the cross-section images of membranes. The results showed that the amorphous regions intercalated with flat plane in the cross-sectional image at micro level as an illustration for the semi-crystalline structure of PVA [40]. For PM membrane, ordered regions were clearly viewed with ordered chains (Fig. 1d & f). While the predominance of amorphous regions was observed in PA membrane. The co-addition of agar and maltodextrin showed compact structure with no amorphous phase observed in Fig. 1h.

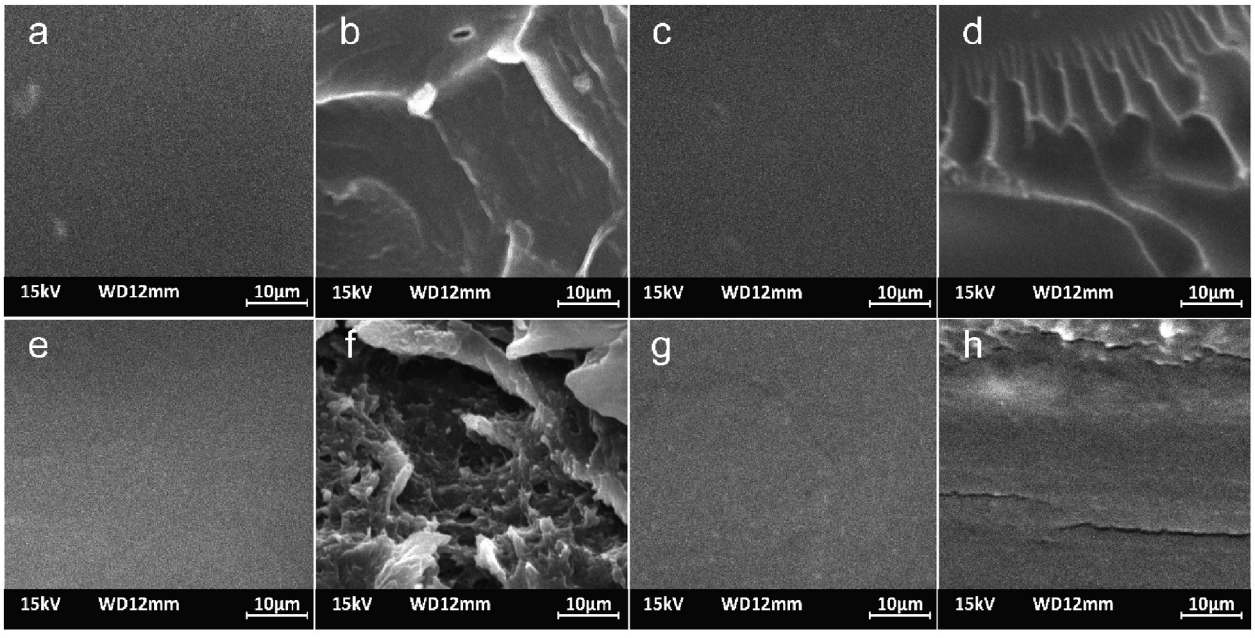

Fig. 1. The surface image at micro-level and cross-section morphology of (a, b) PVA; (c, d) PM; (e, f) PA and (g, h) PAM membrane.

The ATR/FTIR spectra of membranes were shown in Fig. 2. In control PVA spectrum, the characteristic peaks of PVA structure were at 3289 cm^{-1} and 1427 cm^{-1} which were thought to O—H stretching and bending vibrations. The C—H vibration of alkane group was recorded at 2919 cm^{-1} . The peak at 1724 cm^{-1} was signed to C═O stretching vibration of remaining acetate group of PVA after partial hydrolysis process. The C—H group vibration and C—O group stretching vibration were respectively recorded at1245 cm^{-1} and 1083 cm^{-1} [41,42]. The incorporation of only maltodextrin induced a decrease in intensity of peaks at 3289 cm^{-1}, 1724 cm^{-1}, and 1245 cm^{-1} which are closely related to O—H, C═O and C—O vibration. Furthermore, there is a peak shift from 1083 cm^{-1} (C—O group stretching vibration) to 1015 cm^{-1}. These changes were evidence for the presence of hydrogen interaction between —OH groups of PVA and maltodextrin. The similar observations were found in the PA spectrum, indicating intermolecular hydrogen-bonding interactions between hydroxyl of PVA and ether linkages in agar backbone alternated intramolecular hydrogen bonding between hydroxyl groups in PVA [43,44]. Interestingly, the co-incorporation of agar and maltodextrin induced to pronounced peak shift. For instance, it can be seen the shift of peaks from 1724 cm^{-1}, 1427 cm^{-1}, 1245 cm^{-1}, and 1083 cm^{-1} to new positions at 1609 cm^{-1}, 1350 cm^{-1}, 1148 cm^{-1} and 1015 cm^{-1} which are signed to C═O, O—H, C—H, and C—O group vibration. Moreover, the peak intensity of O—H group considerably decreased and became flatter compared to other samples. These changes confirmed that the synergistic effect of agar and maltodextrin in the crosslinking process hydrophilic hydroxyl groups in PVA chains.

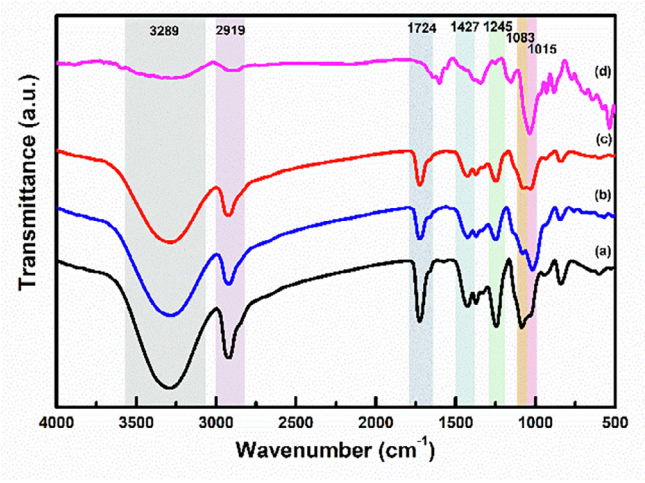

Fig. 2. The ATR/FTIR of (a) PVA, (b) PM, (c) PA and (d) PAM membranes.

The thermal property of blend membranes was assessed by TGA and DTG analysis as seen in Fig. 3. As observed, the mass loss of control PVA membrane occurs in separate stages including 70–170 °C, 270–380 °C, and 405–500 °C. The initial mass loss of the membrane was likely due to the vaporization of water on the PAM membrane surface. The mass reduction at the second stage is ascribed to the main decomposition of PVA [11,18,22,23]. The mass reduction in the final stage resulted from the decomposition of carbon–carbon chains [39]. Remarkably, by adding maltodextrin and agar to PVA membranes, a new mass loss appeared at 243–264 °C which is thought to the degradation of maltodextrin [24,25]. In addition, in the DTG profiles of PAM membrane, the mass loss of main chain was found to be 328 °C which was slight lower compared to those in control PVA membrane (331 °C). Hence, indicating that the thermal degradation of the PAM membrane did not change significantly with the co-combination of agar and maltodextrin.

The angle contact was used to well-describe the surface hydrophilicity/hydrophobicity. It is worth noting that the smaller contact angles provide higher hydrophilicity, while the wider contact angles represent lower hydrophilicity [11,20,21]. The contact angle values were recorded below 45° for PVA and PM membranes, indirectly indicating their hydrophilic property. The contact angle value increased to 50° on the addition of only agar, illustrating the more hydrophobic property of PA membrane compared to control PVA. Interestingly, PAM membrane exhibited the great water resistance compared to others, corroborated by contact angle values >90°. Therefore, a decrease in the affinity toward water of PAM membrane can be expected that they provide selective adsorption for dye molecules higher than water molecules.

The degree of swelling of the membranes was linked to crosslinking density occurring in polymeric network, which significant effects on dye removal performance. Visually, it was observed that

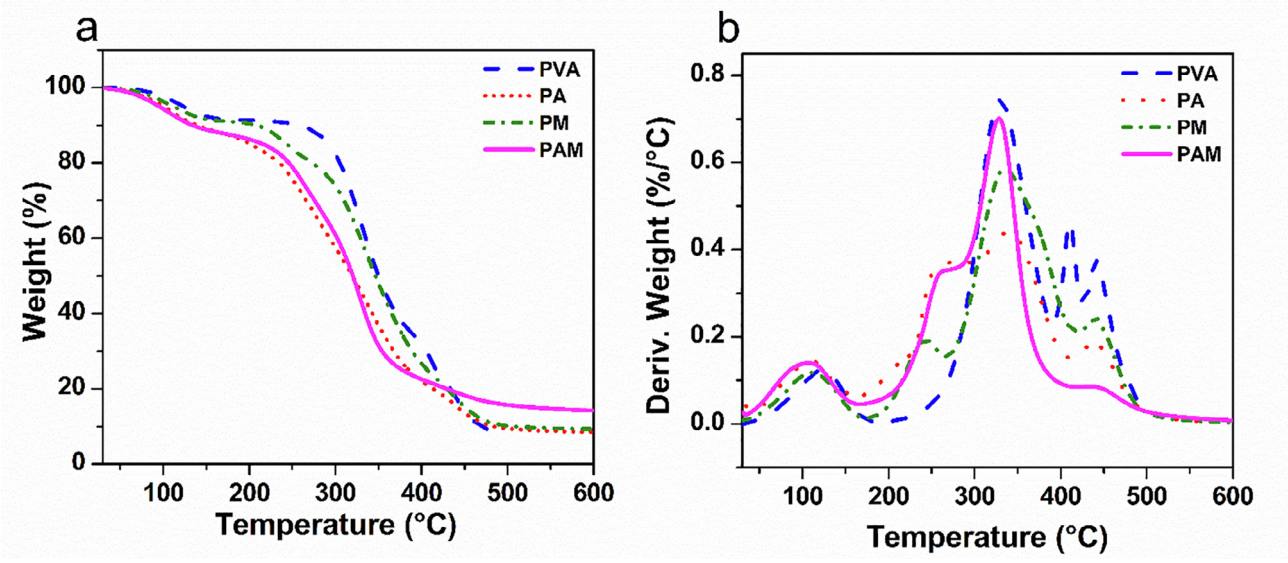

Fig. 3. The (a) TGA and (b) DTG profiles of PVA, PM, PA and PAM membranes.

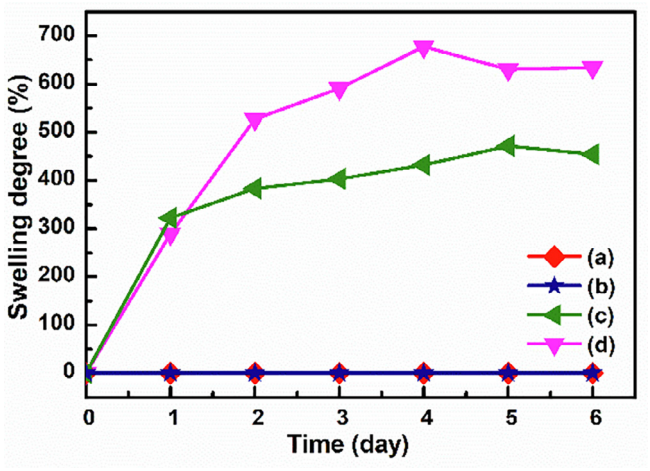

Fig. 4. The swelling percentage of (a) PVA, (b) PM, (c) PA and (d) PAM membrane was measured at room temperature (27 °C) for 6 days.

control PVA and PM were completely dissolved while PA and PAM membranes became rubbery when they were soaked in water. For PA membrane, the swelling degree rapidly increased in first 24 h (Fig. 4) because water molecules easily released into hydrophilic channels resulting in the relax of hydrated polymeric chains and the volume in polymeric network was then expanded in water [44]. Subsequently the diffusion of water in such channels reached the equilibrium because the space in polymeric was fully occupied. Compared to PA, the degree of swelling of PAM membrane showed a much higher increase and hit the peak after 4 days and kept stable for further increasing time. This outcome indicated that the co-addition of agar and maltodextrin prevents complete solubility of PVA due to hydrogen-bonding interaction between —OH groups of PVA, agar and maltodextrin chains and much free volume in polymeric network was found in PAM membrane in comparison with PA.

3.2. The adsorption capacity of membrane

Effect of factors including exposure time between adsorbates and adsorbents, solution pH and initial CV concentration was depicted in Fig. 5. As seen in Fig. 5a, the adsorption capacity of PAM membrane for CV uptake rapidly increased within first 50 mins and then steadily increased before reaching the equilibrium after 210 mins exposure. The high initial adsorption rate

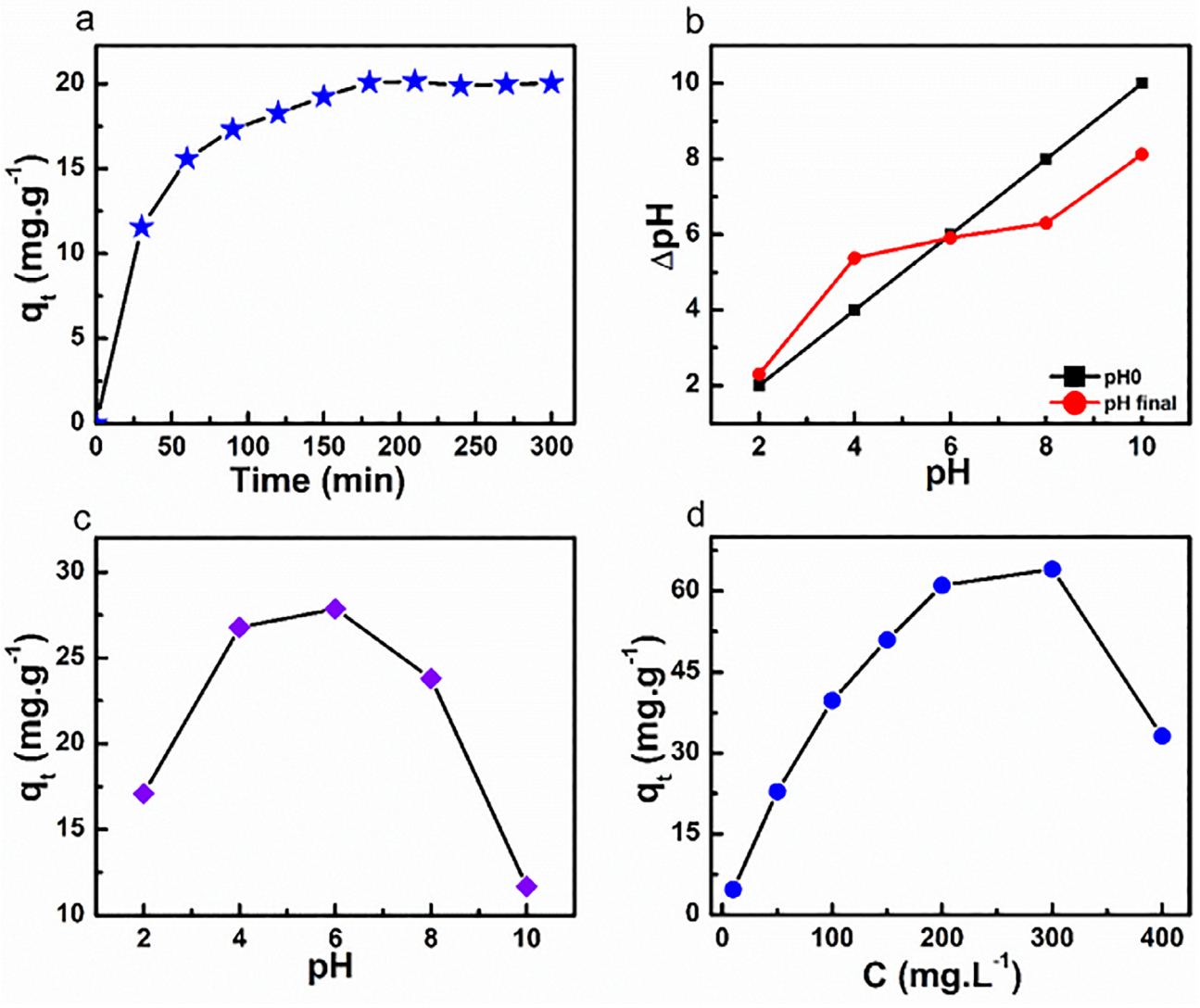

Fig. 5. The effect of (a) contact time, (b) pH_{pzc}, (c) solution pH and (d) CV concentration to the CV adsorption of PAM membrane.

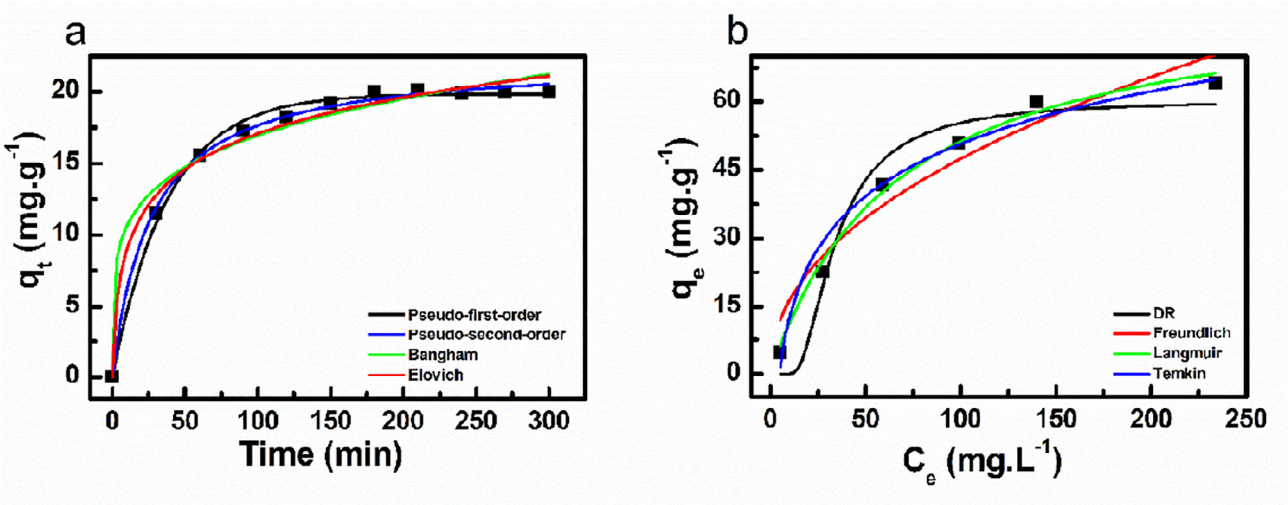

Fig. 6. (a) The Adsorption Kinetics and (b) The Adsorption Isotherms.

was likely based on the large number of active sites available on the PAM membrane surface which likely interacted with CV molecules. After 50 mins, the fully occupied sites by CV molecules on the surface exerted an obstruction in the interaction between the active sites and CV molecules and resulting in a slow adsorption rate. Based on the results, the equilibrium time was 210 mins used for further experiments.

The solution pH is the key to the CV adsorption process because it is closely associated with the charge on the PAM surface and the ionization level of CV molecules. As early reported, the pH_z was closely related to electrostatic repulsion [42]. The pH_z value which usually indicated as solution condition at net surface charge equal to zero, was determined and recorded at 5.87 (Fig. 5b). It means that if the pH value is below 5.87, the membrane surface with negative charge is found and conversely, if the pH value is over 5.87, the membrane surface is positively charged. The influence of the pH media on the CV uptake was performed at the pH range of 2 – 10 (Fig. 5c). The maximum amount of CV adsorption on the PAM membrane attained 28.87 mg·g^{-1} at pH = 6. This can be explained that in the acidic media, the adsorption capacity of PAM membrane for CV molecules decreased on the ground of the excessive presence of H^+ ions leading to the competition between the positively charged CV molecules and H^+ ions, resulted in the reduction of the CV adsorption capacity on PAM membrane. The optimum uptake capacity was obtained at pH = 6 because at this pH media, negatively charged PAM membrane surface probably may attract CV dye ions leading to the rise in the adsorption efficiency. The further increase in solution pH resulted in more alkaline medium and high viscosity likely hindering the CV uptake of PAM membrane. Briefly, the highest adsorption capacity was found at pH = 5 which was used for the next experiments.

Evaluating the effect of initial CV concentration on the uptake capacity of PAM membrane was assessed from 10 mg·L^{-1} to 400 mg·L^{-1} as seen in Fig. 5d. The amount of adsorbed CV dyes increases from 2.74 mg·g^{-1} to 71.17 mg·g^{-1} with increasing the initial CV concentration from 10 mg·L^{-1} to 300 mg·L^{-1}. This behavior can be explained that at higher dye concentration, the necessary driving force resulted in the decrease in mass transfer resistances of dye molecules in aqueous solution containing PAM membrane and thus allows to considerably increase the amount of adsorbed dye [6]. However, the uptake capacity decreased on the ground of the saturation of adsorption points at continuously increasing concentration.

3.3. Adsorption kinetics and isotherms

The kinetic curves of PAM membrane for CV adsorption process are illustrated in Fig. 6a and calculated kinetic parameters are presented in Table 1. The R^2 correlation coefficients were documented in following order as follows: Pseudo-second order (0.997)

Table 1
The adsorption kinetic parameters of PAM membrane for CV.

Adsorption kinetics	Kinetic parameters	
Pseudo-First-Order	k_1 (min^{-1})	0.0261
	q_1 (mg·g^{-1})	19.856
	R^2	0.994
Pseudo-Second-Order	k_2 (g.(mg.min)$^{-1}$)	0.002
	q_2 (mg·g^{-1})	22.335
	R^2	0.997
Elovich	β (g.mg^{-1})	0.273
	α (mg.(g.min)$^{-1}$)	3.829
	R^2	0.984
Bangham	k_B(mL.(g.L)$^{-1}$)	6.645
	α_B	0.203
	R^2	0.976

Table 2
The adsorption isotherm parameters of PAM membrane for CV.

Adsorption Isotherms	Isotherm parameters	
Langmuir	k_L(L.mg^{-1})	0.015
	q_m (mg·g^{-1})	84.618
	R^2	0.990
	R_L	0.182
Freundlich	k_F(mg.(g.(mg.L^{-1})$^{1/n}$)$^{-1}$)	5.649
	1/n	0.462
	R^2	0.924
Temkin	k_T (L.g^{-1})	0.212
	B_T(Mol^2).(Kj^2)$^{-1}$	16.607
	R^2	0.969
	b (L.mol^{-1})	151.692
D – R	k_{DR} (Mol^2).(Kj^2)$^{-1}$	143.057
	q_{DR}(mg·g^{-1})	60.364
	R^2	0.950
	E	0.059
	ε	41.391

> Pseudo-first order (0.994) > Elovich (0.984) > Bangham (0.976). This outcome indicated that the Pseudo-second order model is good correlation with adsorption process of PAM membrane for CV dye, as evidenced by the highest correlation coefficient. This may be suggested that the CV adsorption on the PAM membrane is controlled initially by the chemical process [39]. However, the Pseudo-first order also provided high correlation coefficient suggesting that diffusion mechanism likely contribute to the overall mechanism of CV adsorption process by PAM membrane.

The non-linear curves of the isotherm models were observed in Fig. 6b and isotherm parameters were calculated as seen in Table 2. After calculating and fitting, it can be pronouncedly viewed that the Langmuir model was well-fitted with the CV adsorption on PAM membrane with highest R^2 correlation coefficient ($R^2 = 0.990$) meanwhile the R^2came from Freundlich, Temkin and DR models were found in 0.924, 0.969 and 0.950, respectively. These results suggested that CV adsorption process on PAM membrane due to homogeneous monolayer coverage. The maximum amount of CV adsorption was calculated at 84.618 $mg{\cdot}g^{-1}$. The R_L value is 0,182 between 0 and 1 likely suggesting the favorable adsorption.

4. Conclusion

The obtained results showed the successful removal of crystal violet using PVA/agar/maltodextrin membrane. The contact time between adsorbates and adsorbents, solution pH, and intimal CV concentration significantly affected on the adsorption capacity of PAM membrane for CV removal. The maximum amount of CV uptake was found in 84.618 $mg{\cdot}g^{-1}$. The adsorption process was well-obeyed with pseudo-second order kinetic and Langmuir isotherm model. These outcomes provided promising potential for the elimination of organic dyes using PVA-based environment-friendly membrane.

CRediT authorship contribution statement

Bich Ngoc Hoang: Writing - original draft, Writing - review & editing, Supervision, Methodology. **Thuong Thi Nguyen:** . **Dai Van Nguyen:** . **Lam Van Tan:** Writing - original draft, Writing - review & editing.

Declaration of Competing Interest

The authors declare that they have no known competing financial interests or personal relationships that could have appeared to influence the work reported in this paper.

Acknowledgements

This research was supported by a grant from Foundation for Science and Technology Development Nguyen Tat Thanh University (2020.01.027/HĐ-KHCN).

References

[1] D.A. Yaseen, M. Scholz, Int. J. Environ. Sci. Technol. 16 (2019) 1193–1226.
[2] S. Mani, R.N. Bharagava, in: Rev. Environ. Contam. Toxicol. Vol. 237, 2016, pp. 71–104.
[3] C.C. Chen, W.C. Chen, M.R. Chiou, S.W. Chen, Y.Y. Chen, H.J. Fan, J. Hazard. Mater. 196 (2011) 420–425.
[4] K. Mohanty, J.T. Naidu, B.C. Meikap, M.N. Biswas, Ind. Eng. Chem. Res. 45 (2006) 5165–5171.
[5] R. Fabryanty, C. Valencia, F.E. Soetaredjo, J.N. Putro, S.P. Santoso, A. Kurniawan, Y.-H. Ju, S. Ismadji, J. Environ. Chem. Eng. 5 (2017) 5677–5687.
[6] M.R. Kulkarni, T. Revanth, A. Acharya, P. Bhat, Resour. Technol. 3 (2017) 71–77.
[7] J. Nasiri, E. Motamedi, M.R. Naghavi, M. Ghafoori, J. Hazard. Mater. 367 (2019) 325–338.
[8] A. Djelad, A. Mokhtar, A. Khelifa, A. Bengueddach, M. Sassi, Int. J. Biol. Macromol. 139 (2019) 944–954.
[9] E.S. Mansor, H. Abdallah, A.M. Shaban, J. Environ. Chem. Eng. 8 (2020) 103706.
[10] M. Rahmat, A. Rehman, S. Rahmat, H.N. Bhatti, M. Iqbal, W.S. Khan, S.Z. Bajwa, R. Rahmat, A. Nazir, J. Mater. Res. Technol. 8 (2019) 5149–5159.
[11] R. Cherrak, M. Hadjel, N. Benderdouche, M. Adjdir, A. Mokhtar, K. Khaldi, A. Sghier, P.G. Weidler, Silicon 12 (2020) 927–935.
[12] S. Jana, M.K. Purkait, K. Mohanty, Appl. Clay Sci. 50 (2010) 337–341.
[13] S. Hamidzadeh, M. Torabbeigi, S.J. Shahtaheri, J. Environ. Heal. Sci. Eng. 13 (2015) 8.
[14] M. Sarabadan, H. Bashiri, S.M. Mousavi, Korean J. Chem. Eng. 36 (2019) 1575–1586.
[15] P. Monash, R. Niwas, G. Pugazhenthi, Clean Technol. Environ Policy 13 (2011) 141–151.
[16] P. Monash, G. Pugazhenthi, Sep. Sci. Technol. 45 (2009) 94–104.
[17] G. Crini, Bioresour. Technol. 97 (2006) 1061–1085.
[18] S. Karimi, M. Tavakkoli Yaraki, R.R. Karri, Renew. Sustain. Energy Rev. 107 (2019) 535–553.
[19] T. Gaaz, A. Sulong, M. Akhtar, A. Kadhum, A. Mohamad, A. Al-Amiery, Molecules 20 (2015) 22833–22847.
[20] M. Kokabi, M. Sirousazar, Z.M. Hassan, Eur. Polym. J. 43 (2007) 773–781.
[21] T.M.R. Miranda, A.R. Gonçalves, M.T.P. Amorim, Polym. Int. 50 (2001) 1068–1072.
[22] H. Gao, H. Yang, J. Appl. Polym. Sci. 134 (2017) 45324.
[23] D. Ghemati, D. Aliouche, J. Appl. Spectrosc. 81 (2014) 257–263.
[24] K.C.S. Figueiredo, T.L.M. Alves, C.P. Borges, J. Appl. Polym. Sci. 111 (2009) 3074–3080.
[25] T. Miyazaki, Y. Takeda, S. Akane, T. Itou, A. Hoshiko, K. En, Polymer (Guildf). 51 (2010) 5539–5549.
[26] Y. Zhang, P.C. Zhu, D. Edgren, J. Polym. Res. 17 (2010) 725–730.
[27] Y. Cheng, H. Lin, Z. Chen, M. Megharaj, R. Naidu, Ecotoxicol. Environ. Saf. 83 (2012) 108–114.
[28] A. Papancea, S. Patachia, R. Dobritoiu, J. Appl. Polym. Sci. 132 (2015).
[29] G.R. Mahdavinia, A. Massoudi, A. Baghban, E. Shokri, J. Environ. Chem. Eng. 2 (2014) 1578–1587.
[30] B.N. Hoang, T.T. Nguyen, Q.P.T. Bui, L.G. Bach, D.N. Vo, C.D. Trinh, X. Bui, T.D. Nguyen, J. Appl. Polym. Sci. (2019) 48904.
[31] I.M. Jipa, A. Stoica-Guzun, M. Stroescu, LWT 47 (2012) 400–406.
[32] S.M. Lalhmunsiama, D. Lee, Tiwari Chem. Eng. J. 225 (2013) 128–137.
[33] K.W. Kolasniski, in: 2001.
[34] G. Blanchard, M. Maunaye, G. Martin, Water Res. 18 (1984) 1501–1507.
[35] S. Roginsky, Y.B. Zeldovich, Acta Phys. (1934) 554.
[36] E. Tütem, R. Apak, Ç.F. Ünal, Water Res. 32 (1998) 2315–2324.
[37] I. Langmuir, J. Am. Chem. Soc. 40 (1918) 1361–1403.
[38] H. Freundlich, Z. Phys. Chem. 57U (1907).
[39] M.M. Dubinin, in: 1947.
[40] K. Lee, K. Jeoung, D.K. Lee, Y.B. Ji, M. Seo, Y.M. Huh, J.S. Suh, S.J. Oh, Infrared Phys. Technol. 93 (2018) 154–157.
[41] R. Sabarish, G. Unnikrishnan, Carbohydr. Polym. 199 (2018) 129–140.
[42] S. Mallakpour, S. Rashidimoghadam, Polymer (Guildf). 160 (2019) 115–125.
[43] S.T.J. Madera, D. Robledo, P.Y. Freile, Mar. Biotechnol. 13 (2011) 793–800.
[44] J.G. Lyons, L.M. Geever, M.J.D. Nugent, J.E. Kennedy, C.L. Higginbotham, J. Mech. Behav. Biomed. Mater. 2 (2009) 485–493.